The Use of RF Waves in Space Propulsion Systems

E.A. Bering, III
F. Chang-Diaz
J. Squire

Abstract

This paper will review the ways in which RF and microwave radiation may be used in the design of electric propulsion systems for spacecraft. RF power has been used or proposed in electric propulsion systems to ionize, to heat, and to accelerate the propellant, or to produce plasma used to inflate a magnetic field for solar-sail purposes. Direct RF propulsion using radiation pressure or ponderomotive forces is impractical, owing to efficiency considerations. Examples of various systems that have been developed or proposed will be reviewed. The variable specific impulse magneto-plasma rocket (VASIMR) uses RF for producing, heating, and accelerating plasma. Inductive RF and microwave ion thruster schemes use electromagnetic waves to ionize the plasma, which is then accelerated by use of dc grids. The details of the VASIMR, an inductive RF thruster, and a microwave ion thruster are discussed and contrasted with related RF systems.

1. Introduction

The exploration of the solar system will be one of the defining scientific tasks of the new century. One of the obvious challenges faced by this enterprise is the scale size of the system under study: 10^{10} to 10^{12} m. Over distances on this scale, the mission designer is faced with the choice of accepting multi-year or even decadal mission timelines, paying for enormous mass ratios, or finding a way to improve on the performance of today's chemical rockets. For human space flight beyond Earth's orbit, medical, psychological, and logistical considerations all dictate that drastic thruster improvement is the only choice that can be made. Even for robotic missions beyond Mars, mission timelines of years can be prohibitive obstacles to success, meaning that improvements in deep-space sustainer engines are of importance to all phases of solar-system exploration [1]. For reasons that will be discussed below, improvement in thruster performance can best be achieved by using an external energy source to accelerate or heat the propellant [2]. This paper will review the use of radio frequency (RF) and microwave electromagnetic radiation as one of the methods for feeding electrical energy into the working fluid or propellant of spacecraft propulsion systems.

1.1 The Need for Electric Propulsion

The so-called "rocket equations" are presented as examples in most elementary physics texts. The change in velocity, Δv, that can be obtained from any rocket engine is given by

$$\Delta v = u \ln \frac{M_i}{M_f}, \qquad (1)$$

where u is the exhaust velocity of the rocket motor, M_i is the initial mass of the fully fueled rocket with payload, and M_f is the final mass of the payload and empty rocket motor. The fact that the logarithm is a very weak function imposes a large mass and cost penalty on any mission that needs a Δv that is a large multiple of the exhaust velocity. The obvious solution is to find ways to increase the exhaust velocity, u, or the specific impulse, $I_{sp} = u/g$, of thrusters intended for use as deep-space sustainer engines, where g is the acceleration owing to gravity at the Earth's surface.

The fundamental obstacle to increasing the specific impulse of chemical rockets lies in thermodynamics. Chemical rockets are heat engines. The energy per molecule that is available to become kinetic energy of the exhaust is limited to the amount of Gibbs free energy per molecule available in the reaction, which is on the order of an eV or

Edgar A. Bering, III is with the University of Houston, Departments of Physics and Electrical and Computer Engineering, 617 Science and Research I, Houston, TX 77204-5005, USA; E-mail: eabering@uh.edu.
Along with Franklin Chang-Díaz and Jared Squire, he is also with the Advanced Space Propulsion Laboratory, NASA Johnson Space Center, 13000 Space Center Blvd., Houston, TX 77059, USA.

This is one of the invited *Reviews of Radio Science*, from Commission H.

less. Furthermore, most of the available energy goes into heating the exhaust gas. The nozzle then converts some of this heat energy into the kinetic energy of thrust, a process that is inexorably constrained to be inefficient by the Second Law of Thermodynamics. Thus, the best chemical rockets have I_{sp} ~ 350-460 s. All rockets, including electric propulsion systems that operate as heat engines using a physical mechanical nozzle, ultimately encounter very similar thermodynamic limits, since the real limit is the need not to melt the nozzle material. The energies required to break the chemical bonds in refractory nozzle materials are on the same order as the combustion energies. Consequently, externally heated thermal rocket designs with mechanical nozzles can only achieve I_{sp} ~ 800-1000 s. For piloted missions to Mars and any type of short-duration mission to the outer planets, I_{sp} ~ 3000-30000 s will be required [3-5]. This requirement means that one must find a method to accelerate the propellant that uses an external energy source, and either keeps the propellant away from contact with solid nozzle walls, or uses a non-thermal method of acceleration. The only non-thermal energy source available on spacecraft is the vehicle's electric power system, which means that deep-space sustainer engines are going to be electric propulsion systems of one type or another. Electric propulsion systems have the added advantage that many of the systems now under development either magnetically confine the propellant, or use non-thermal acceleration mechanisms that avoid the need for mechanical nozzles, or both.

Radio frequency or microwave electromagnetic waves have found a number of uses in electric propulsion systems. The basic motivation is to provide a method of injecting energy into the propellant gas that does not require use of electrodes that are in contact with the gas, in order to avoid life-time-limiting erosion problems with said electrodes. The purpose of this paper is to review some of the more important types of RF and microwave electric propulsion system designs.

2. Electric Propulsion Systems

2.1 Classification Schemes

There are two ways that one may classify RF electric thrusters. There is a classification scheme that applies to all types of electric thrusters, which is based on their physical method of operation [6]. One may also organize RF systems according to how the RF energy is used.

2.2 Physical Method of Operation

There are three main categories of the method of operation for electric thrusters: electrothermal, electrostatic, and electromagnetic [6]. Electrothermal thrusters are examples of what were referred to as externally heated thermal thrusters, above. Electric power is used to heat the propellant material, which then expands and exhausts through a conventional mechanical nozzle to produce thrust. Examples include resistojets and arcjets. Electrostatic thrusters produce thrust by allowing positively charged ions to enter a region containing a large dc electric field, which accelerates the ions. Examples include gridded ion engines, Hall-effect thrusters, and field-emission thrusters. Electromagnetic thrusters produce thrust by applying electromagnetic forces to the propellant. Examples include magnetohydrodynamic (MHD) thrusters, ponderomotive thrusters, and the variable specific impulse magneto-plasma rocket (VASIMR).

2.3 Role of RF Energy in Thruster Operation

One may also characterize RF electric thrusters in terms of the role that the RF energy plays in the operation of the thruster. RF or microwave energy may play one or more of four roles in thruster operation: plasma ionization, propellant heating, propellant acceleration, or direct thrust production. In this context, the term "heating" refers to any stochastic energy injection process that obeys the principle of equipartition of energy. In contrast, the term "acceleration" will be used to refer to any more deterministic process that preferentially supplies energy to a selected kinetic degree of freedom. Plasma ionization RF thrusters utilize the RF to ionize the propellant, or working fluid. Almost all RF thrusters fall in this category. Several ion thruster schemes use RF or microwave ionization sources to ionize propellant that is accelerated with an electrostatic potential. At least one thruster design, the mini-magnetosphere plasma propulsion device, uses RF-produced plasma to inflate a magnetic solar-wind sail. Plasma heating by RF or microwave is used to heat plasma in microwave electrothermal thrusters (MET).

Acceleration of plasma that has been produced in an RF or microwave source can be accomplished by use of grid-produced electrostatic fields, by ambipolar electrostatic fields that are self-consistently generated in plasmas that have elevated electron temperatures, or by ion-cyclotron resonant heating (ICRH), which is misnamed since the kinetic energy is injected preferentially into a single degree of freedom. The ICRH name and acronym will be retained, owing to the name recognition of the terminology in the fields of fusion energy and auroral physics. Examples of gridded ion thrusters with RF or microwave sources include the RF ion thruster assembly (RITA) on ESA's ARTEMIS spacecraft [7, 8], and the microwave electron-cyclotron resonance (ECR) thruster on the Japanese asteroid-sample return mission, Hayabusa (MUSES-C) [9, 10]. Relatively large ambipolar electrostatic fields are produced in the exhaust plume of magnetized RF plasma sources, because these devices typically produce plasmas with large electron pressure gradients, and $T_e > T_i$, where T_e is the electron temperature and T_i is the ion temperature. Examples of

thrusters that use ambipolar acceleration include the whistler-wave plasma thruster [11, 12] and stand-alone helicon thrusters [13-15]. VASIMR is both an example of a system that uses ion-cyclotron resonant heating to accelerate ions, and an example of a system that can be operated as an ambipolar acceleration thruster [16, 17].

Direct thrust production refers to methods that utilize either direct photon thrust, or a ponderomotive interaction with the ambient magnetospheric or solar-wind plasma. Owing to the inherent energy inefficiency of these approaches, no such thrusters are presently under development. These methods will only be practical for ultra-power-rich missions with severe mass ratio constraints.

2.4 Specific Systems

Three systems will be examined in some detail. The two space-qualified systems, RITA on ARTEMIS and the microwave electron-cyclotron resonance thruster on Hayabusa, merit detailed discussion because of their pedigree and history. The VASIMR engine will be discussed in detail for several reasons. It is the system that is best suited to scaling up to megawatt power levels. It is the only two-stage RF system under development. Finally, it is the system that the authors know best.

This paper will briefly mention all of the other major RF- or microwave-using electric thruster systems now under development. There is one electrothermal concept, the microwave electrothermal thruster (MET). There are two ambipolar devices, the whistler wave and helicon thrusters. M2P2 is the only concept in the "other" category.

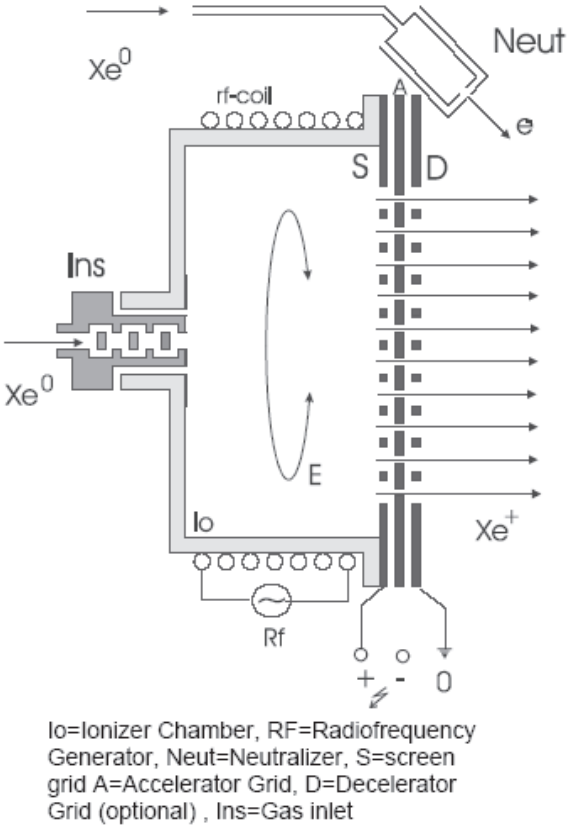

Figure 1. A cartoon schematic of the RF ion thruster (RIT), illustrating the operating principle ([20, 31]; Copyright © 2003 by EADS Space Transportation GmbH; reproduced with permission.)

2.4.1 RF-Ion Thruster (RIT)

The RF-ion thruster (RIT) has been under development for more than thirty years at the University of Giessen and at EADS Space Transportation (formerly astrium GmbH, MBB, and Dasa) [18]. The operating principle is the use of an inductive plasma discharge to ionize the propellant (presently xenon). A cylindrical solenoid coil surrounds an electrically non-conducting plasma chamber (Figure 1) [7, 19, 20]. This coil is driven by a 0.7-1 MHz RF signal. The coil produces an axial magnetic field and an azimuthal electric field in the plasma chamber. The azimuthal electric field accelerates the plasma electrons, which ionize the propellant by impact ionization. The plasma ions are then extracted from the chamber and accelerated by means of an electrostatic field, which is applied by means of a three-grid exhaust aperture.

The fundamental electrodynamic principles of operation of this device are very simple, owing to the fact that the plasma is not magnetized. There are two factors critical to the operation of the system that determine the operating frequency. Ionization efficiency maximizes when the neutral pressure in the discharge chamber is such that the electron-neutral collision frequency is equal to the input RF power. In order to penetrate the plasma, the RF input frequency must remain above the local plasma frequency. If the input flow rate of the propellant and the available RF power are sufficient to produce a plasma density such that the plasma frequency approaches the operating frequency, skin-depth effects will act to limit the penetration of the wave into the plasma and to reduce the ionization efficiency of the thruster. In effect, the device is operated in a low plasma density regime, where single-particle dynamics suffice to explain its operation.

The RIT-10 has an impressive pedigree. A qualification model has been operated for nearly 19000 hours in a laboratory qualification test [21-23]. The first space test of the RIT-10 assembly (RITA) was on the EUropean REtrievable CArrier Assembly (EURECA) [19, 24]. This experimental prototype operated at thrust levels of 5-10 mN for 240 hours before a solder joint on the input to the RF coil melted, terminating operation.

The first operational use of the RIT-10 was on the European Space Agency's Advanced Relay Technology Mission (Artemis) spacecraft. This geosynchronous

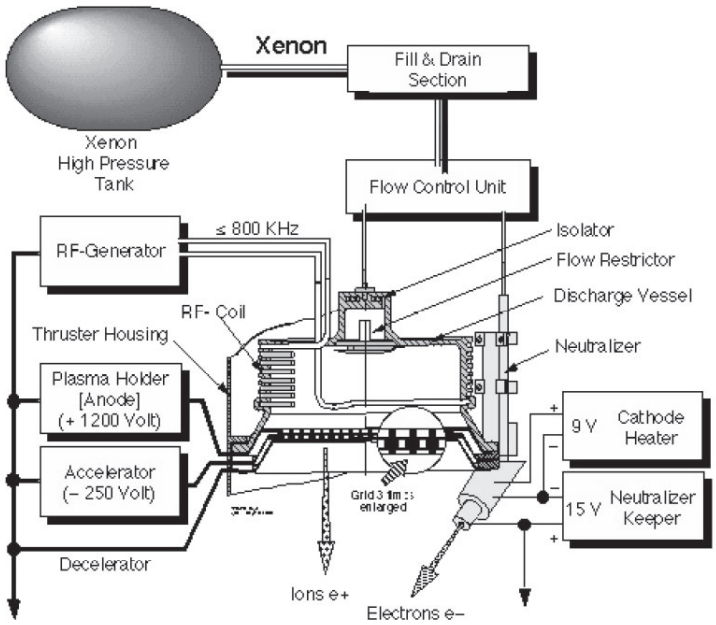

Figure 2. A block diagram of the RF ion thruster ([25, 28] copyright © 2001 astrium GmbH; reproduced with permission).

spacecraft was equipped with four ion thrusters, including two RITAs in order to perform north-south station keeping [7, 8, 24-27]. The RITA models on this mission had a mass of 15.4 kg each. They produced 15 mN of thrust at a specific impulse of 3400 s, requiring a power input $<$459 W each. It was fortunate for the mission planners that there were ion thrusters on board, because a launcher failure resulted in an initial elliptic orbit that was much lower than intended, leaving the spacecraft with insufficient chemical propulsion fuel to achieve geosynchronous orbit. The chemical apogee boost engine was used to place the spacecraft in a 31,000 km circular parking orbit. From there, the ion propulsion system was used successfully to raise the orbit and to adjust the inclination to a final position close to the nominal location for the mission. Despite the fact that the mechanical integrity of some components was compromised by excessive vibration during the launcher failure, the ion engines proved themselves up to the task. RITA1 had to be shut down after 698 hours of operation owing to a blockage in the xenon gas line. RITA2 operated successfully for 5863 hours. It appears that RITA 2 remains capable of providing station-keeping thrust for the remainder of the 10-year mission [8, 26, 27].

The major advantages of the RF-ion thruster system include the increase in expected lifetime that stems from not having a hollow cathode or other electron-bombardment device operating in contact with the plasma, and the cost reduction associated with not having to develop and qualify a high-current cathode. The major disadvantages are limitations on the upward scalability of the system. The plasma is in contact with the wall of the discharge chamber, which limits total power dissipation. The plasma-frequency or skin-depth problem mentioned above limits the plasma density, fuel flow, and maximum thrust, which means that high thrust and power can only be achieved by increasing thruster area and flying multiple thrusters. A similar constraint is imposed by the need to hold the perveance of the exhaust beam below the threshold for triggering beam plasma discharge instabilities (BPD). The use of grids to provide the electrostatic acceleration imposes a lifetime limit, as a result of grid erosion by sputtering.

In a field that is as new and as rapidly developing as electric spacecraft propulsion, operating hardware is already being re-engineered, upgraded, and improved. The RIT-10 ARTEMIS is no exception to this rule. The system is presently evolving along two separate paths. First, an effort has been made to develop an improved model of the 10-cm diameter RIT-10, known as the RIT-10 EVO (EVOlution), which provides enhanced performance within essentially the same size and weight envelope [18, 20, 25, 28, 29]. The main step taken in this effort was to increase the open-area fraction of the grids, and to improve the ion optics. The results were big increases in the range of available thrust levels or throttle ability. The RIT-10 ARTEMIS was capable of about 10% thrust variation, while the RIT-10 EVO can provide any thrust from 1 mN to 41 mN. The RIT-10 EVO can produce about 10% higher specific impulse, while operating at the same thrust level as the RIT-10 ARTEMIS. It also has reduced acceleration grid current, and reduced specific power consumption.

The other development path is intended to produce a larger thruster, capable of producing 150-200 mN of thrust. The RIT-XT has a beam diameter of 21 cm. The discharge chamber is conical, rather than cylindrical. It can produce 150 mN of thrust, with an input power of 4.5 kW and a specific impulse of ~5000 s, operating at a 2 kV beam voltage. Increased specific impulse at the same thrust level can be accomplished by increasing the beam voltage and power input [18, 20, 28-31].

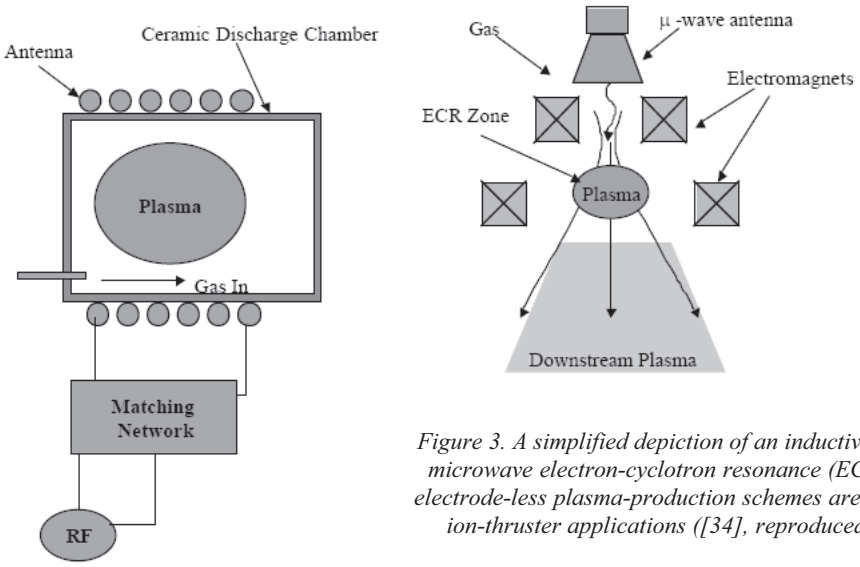

Figure 3. A simplified depiction of an inductive RF discharge and a microwave electron-cyclotron resonance (ECR) discharge. These electrode-less plasma-production schemes are readily adaptable for ion-thruster applications ([34], reproduced with permission).

2.4.2 Microwave Electron-Cyclotron Resonance (ECR) Thruster

The excitation mechanism in inductive RF discharges, such as the RF-ion thruster, is a non-resonant process. It is well known that the selection of a suitable resonance will substantially increase the ability of a propellant to absorb RF energy. The ionization mechanism of most plasma sources is ultimately electron bombardment, which means that RF ionization systems that operate at or near an electron resonance have been extensively investigated. These resonances include the electron-cyclotron resonance (ECR), and the two hybrid resonances, upper and lower. The helicon discharge, which operates near the lower hybrid resonance, will be discussed in subsequent sections. The microwave electron-cyclotron resonance thruster uses a combination of the electron-cyclotron and upper-hybrid resonance to ionize propellant and create an electrodeless cathode [9, 32-34]. A comparison of the RF induction and microwave electron-cyclotron resonance systems is shown in Figure 3 [34].

The electron-cyclotron resonance method of plasma generation has been investigated off and on since the 1960s. The early work ran into problems associated with a lack of lightweight, space-proven microwave sources, and the need for fairly intense magnetic fields, which imposed unacceptable weight penalties using the available magnet technology. By the 1980s, these problems had been solved. The needs of the communications satellite industry have led to the development of several rugged, small, and efficient microwave sources. Superconducting magnets and samarium-cobalt permanent magnets have provided two feasible alternative methods for creating the required magnetic field.

The present generation of microwave electron-cyclotron resonance thrusters traces its heritage to work done by H. Goede at the TRW Space and Technology Group during the early and middle 1980s [32]. Goede designed and tested a 30-cm device with a bucket-type ionization chamber. Two separate families of thrusters have sprung from this initial work. The Japanese Institute of Space and Astronautical Sciences (ISAS) has developed a 10-cm microwave electron-cyclotron resonance thruster

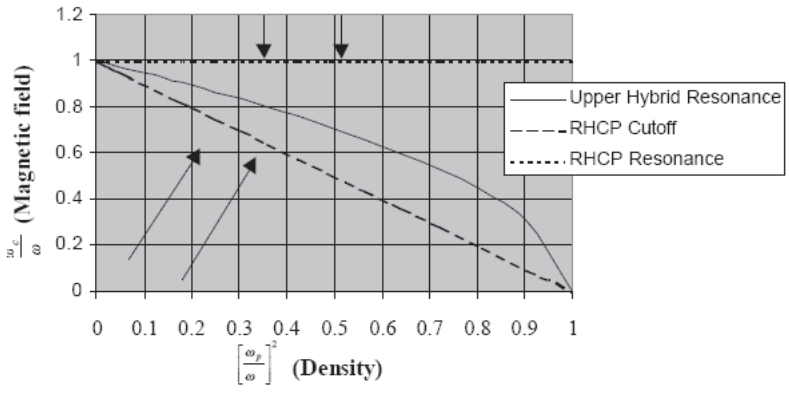

Figure 4. A CMA diagram depicting various resonances and cutoffs for a specified plasma density and magnetic field. The lower two arrows depict waves approaching the electron-cyclotron resonance from the weak-field side, while the upper two depict an approach from the high-field side ([42], reproduced with permission).

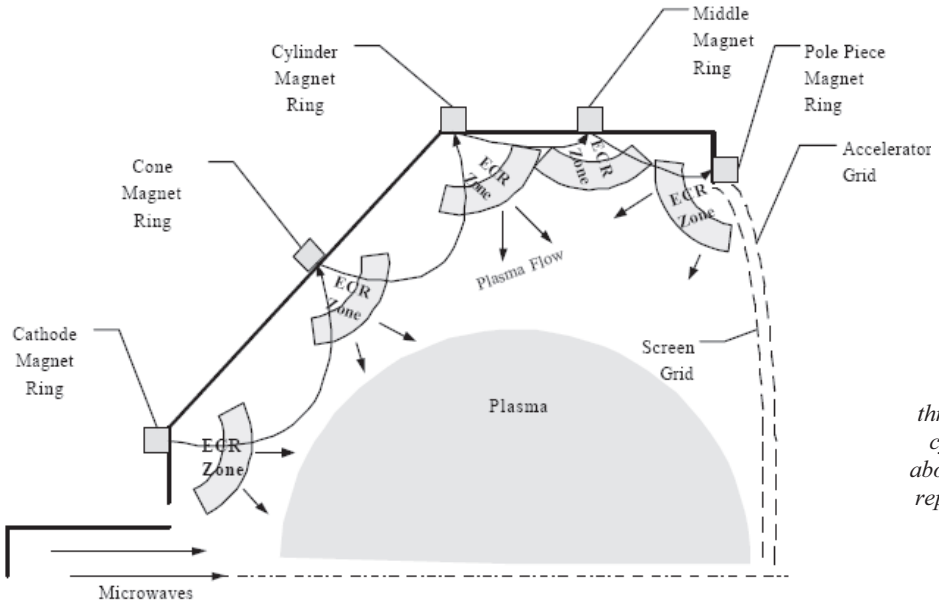

Figure 5. An electron-cyclotron resonance ion thruster. Notice the electron-cyclotron resonance zones above each magnet ring ([34], reproduced with permission).

(the mu-10) that operates at a frequency of 4.25 GHz [9, 10, 33, 35-41]. Four of these engines are presently operating successfully on the Hayabusa (formerly MUSES-C) asteroid sample return mission. A 30-cm size expanded version of the mu-10 is presently under development. A US group at NASA Glenn Research Center is developing a 25 kW microwave electron-cyclotron resonance thruster known as the High Power Electric Propulsion (HiPEP) ion engine [34, 42, NASA Press Release, 2003]. The performance parameters of these systems will be reviewed after we have discussed the physics of the resonance mechanism.

The plasma physics of the electron-cyclotron resonance thruster is subtle and interesting. Actually, the thruster is slightly misnamed, owing to the fact that the upper-hybrid resonance is also excited in many configurations. The electron-cyclotron resonance plasma source operates in regions 1, 2, 3, 6a, and sometimes 7 of the Clemmow-Mullaly-Allis (CMA) diagram, using *Stix* [43] region labeling, as shown in Figure 4. In both the mu-10 and the NASA designs, the microwave power enters the plasma chamber via an axial cylindrical waveguide, as shown in Figure 5 [42].

Circular rings of cup-type permanent magnets are used to create multiple electron-cyclotron resonance zones. This design makes use of the magnetic mirror force to exclude plasma from the microwave inlet region, which means that the waves approach the first electron-cyclotron resonance region from the high-field region. Since the microwave propagation vector, **k**, is parallel to **B** in this region, R-X mode waves have direct access to the electron-cyclotron resonance or RHCP resonance [33, 34]. In multiple-ring configurations, either planar or bucket type, the outer magnets also have associated electron-cyclotron resonance zones [9, 44, 45]. The field geometry in the vicinity of these rings is such that the microwaves approach these electron-cyclotron resonance zones either perpendicular to **B** or at an oblique angle. To reach these resonances, the R-X mode first encounters the $R = 0$ cutoff, which means that it has to tunnel through an evanescent zone to excite the upper-hybrid resonance. It is also possible for the L-O mode to enter a high-field region and to couple to the R-X mode via reflection.

These thrusters have two "modes" of operation, low and high power. In the low-power mode, bright regions of visible emission from the plasma are observed in the predicted plasma-generation zones, with very little emission detectable in the center of the device, and an enhancement of plasma density near the wall [34, 37, 44]. The perpendicular transport process whereby plasma reaches the center is presumed to result from diffusion, but it has not been studied in any detail. In the high-power mode, which has been observed in both US and Japanese studies, the visible emissions from the plasma are uniform across the thruster, showing no visible enhancements at the electron-cyclotron resonance zones [42]. There are two interpretations of this observation. It has been suggested that the uniform glow is the result of an abrupt enhancement in the rate of cross-field diffusion, with most plasma production still occurring in the electron-cyclotron resonance zones [42]. An alternative interpretation is that plasma production is occurring throughout the volume of the discharge chamber by means of the oblique, low-field upper-hybrid resonance [44]. The resolution of this controversy awaits future research.

In general, the need to keep the plasma frequency below the exciting microwave frequency limits the plasma density and, therefore, the total thrust that these devices can produce. This requirement is what dictates the need to operate at the highest practical microwave frequency and magnetic field. The fact that the electrons will gain energy continuously allows the discharge to take place at lower neutral pressures than must be used in the RF-induction thruster. In general, these are self-igniting discharges, which do not require the injection of seed electrons to ignite.

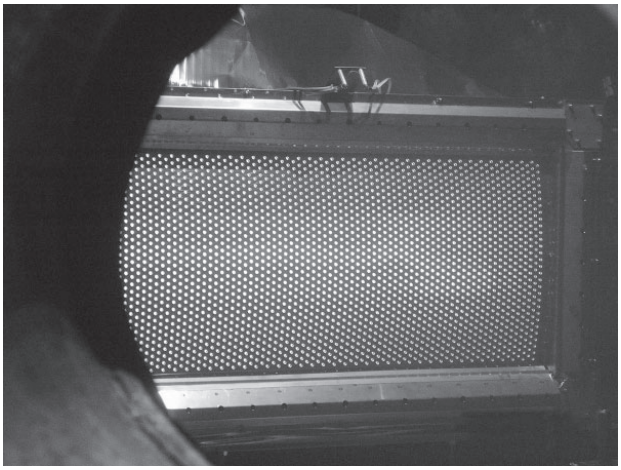

Figure 6. Initial thrust testing of the HiPEP ion engine in a vacuum chamber at NASA's Glenn Research Center (NASA press release).

The Japanese mu-10 microwave electron-cyclotron resonance thruster is one of the two fully space-qualified engines discussed in this review. The Hayabusa asteroid explorer, which was launched on May 9, 2003, is using ion propulsion for cruise phase propulsion. The ion-thruster assembly on Hayabusa consists of four mu-10 engines and associated microwave neutralizer cathodes. Each xenon mu-10 can produce 1.4-7.8 mN of thrust, with a specific impulse between 2687 and 3011 s, using 103-386 W of power each [10]. The prototype model has been endurance tested for 18000 hours [38]. As of December, 2003, the engines had operated successfully for 8147 hours, accomplishing most of the Δv required to enable the Earth-swing-by in June, 2004 [45a].

The NASA program at Glenn Research Center is aimed at high-power mission requirements. The HiPEP ion engine utilizes a microwave electron-cyclotron resonance plasma source and a unique rectangular 41 × 91 cm set of ion optics. The system is intended to be one of the candidate propulsion systems for the Jupiter Icy Moons Orbiter (JIMO) mission. A successful initial test of HiPEP was announced in November, 2003 (NASA press release). During this test, the engine operated at 12 kW, and produced an exhaust with a specific impulse of 6000-8000 s. HiPEP is designed to operate eventually at a full power level of 25 kW. Figure 6 shows a picture of the HiPEP exhaust during the initial testing.

The major advantages of the microwave electron-cyclotron resonance system include the increase in expected lifetime that stems from not having a hollow cathode or other electron-bombardment device operating in contact with the plasma, and the cost reduction associated with not having to develop and qualify a high-current cathode. Lower required amplitude of the excitation wave and lower operating neutral densities are other advantages, along with a reliable self-ignition capability. The major disadvantages are limitations on the upward scalability of the system. The excitation-region plasma can leak out through the mirror region of each magnet via pitch-angle diffusion. This process is an undesirable plasma loss, and also puts a heat load directly on the most heat-sensitive element in the discharge chamber, the Sm-Co magnets. This heat flow severely limits total power dissipation. Efficiency is limited by the difficulty of coupling the TE_{11} waveguide mode in the microwave transmission system exclusively to the R-X mode in the plasma. Any power going into the L-O mode basically represents a power loss. The plasma-frequency problem mentioned above limits the plasma density, fuel flow, and maximum thrust, which means that high thrust and power can only be achieved by increasing thruster area and by flying multiple thrusters. A similar constraint is imposed by the need to hold the perveance of the exhaust beam below the threshold for triggering beam plasma discharge instabilities. The use of grids to provide the electrostatic acceleration imposes a lifetime limit as a result of grid erosion by sputtering.

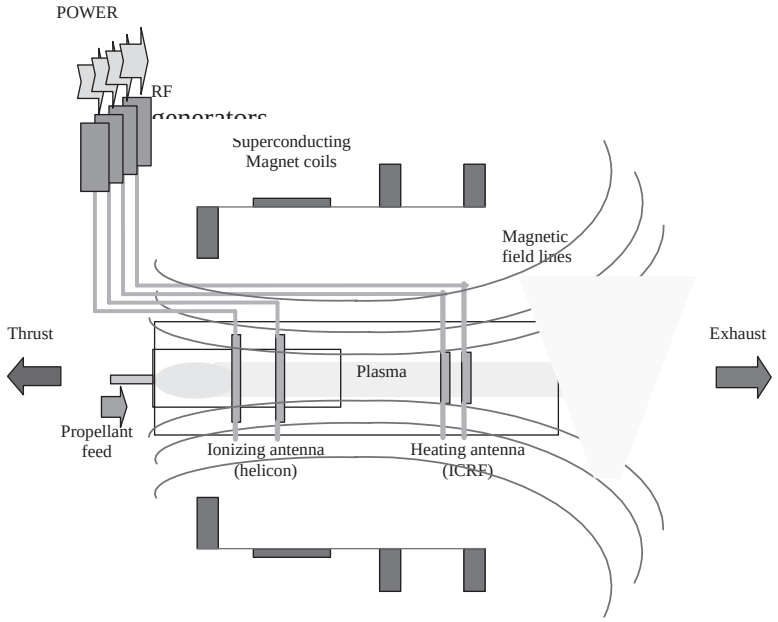

Figure 7. A simplified system schematic of the VASIMR engine ([17]).

2.4.3 Variable Specific Impulse Plasma Rocket (VASIMR)

The problem of wall losses is common to all of the systems that have been discussed so far in this paper. Systems with axial magnetic fields, such as the variable specific impulse plasma rocket (VASIMR), open up new and exciting possibilities for achieving much higher power densities and specific impulses than unmagnetized systems [16, 17, 46-48]. Utilizing ionized gases accelerated by electric and magnetic fields, these devices expand the performance envelope of rocket propulsion far beyond the limits of the chemical rocket. With a properly shaped magnetic duct, the internal energy of plasma can be extracted in the form of rocket thrust, through conservation of the first adiabatic invariant. The duct becomes a magnetic nozzle, the magnetic equivalent of a conventional nozzle. Moreover, the non-physical nature of such a nozzle also suggests an inherent adaptability, which (in analogy to the transmission in an automobile) could continuously tailor the exhaust plume to respond to the conditions of flight. An adaptable nozzle better utilizes the available rocket power, leading to better performance. Although much earlier work identified this benefit, its implementation in chemical rockets with fixed material nozzles proved impractical. In addition, magnetized systems can be designed that have electrode-less ion acceleration mechanisms. VASIMR is an example.

Research on the VASIMR engine began in the late 1970s, as a spin-off from investigations on magnetic diverters for fusion technology [49]. A simplified schematic of the engine is shown in Figure 7. Three linked magnetic stages perform specific interrelated functions. The first stage handles the main injection of propellant gas and its ionization. The second stage, also called the "RF booster," acts as an amplifier to further energize the plasma. The third stage is a magnetic nozzle, which converts the energy of the fluid into directed flow.

The VASIMR consists of three main sections: a helicon plasma source, a radio-frequency (RF) power booster, and a magnetic nozzle. Figure 7 shows these three stages integrated with the necessary supporting systems. One key aspect of this concept is its electrode-less design, which makes it suitable for high power density and long component life by reducing plasma erosion and other material complications. The magnetic field ties the three stages together and, through the magnet assemblies, transmits the exhaust reaction forces that ultimately propel the ship.

VASIMR is an RF-driven device, where the ionization of the propellant is done by a helicon-type discharge [50-52]. The plasma ions are further accelerated in the second stage by ion-cyclotron resonance heating (ICRH), a well-known technique, used extensively in magnetic confinement fusion research. Due to magnetic-field limitations on existing superconducting technology, the system presently favors the light propellants; however, the helicon, as a stand-alone plasma generator, can efficiently ionize heavier propellants, such as argon and xenon.

The physics of the VASIMR engine are being investigated primarily in the VX-10 device at the NASA Johnson Space Center (JSC.) However, supporting investigations are also being carried out at the Oak Ridge and Los Alamos National Laboratories, the University of Texas at Austin, and the NASA Marshall Space Center in Huntsville, Alabama. A trimetric view of the Johnson Space Center device and associated diagnostics is shown in Figure 8. The axial magnetic-field profile is also shown on the lower-right corner of the graph. Present operations use a cusp field at the upstream end of the helicon antenna, but future configurations will move away from this feature.

The helicon first stage is critically important, inasmuch as its performance sets the tone for that of the second stage or RF booster. The helicon discharge uses 25 MHz right-hand-polarized whistler-mode waves (regions 8b and 11 on

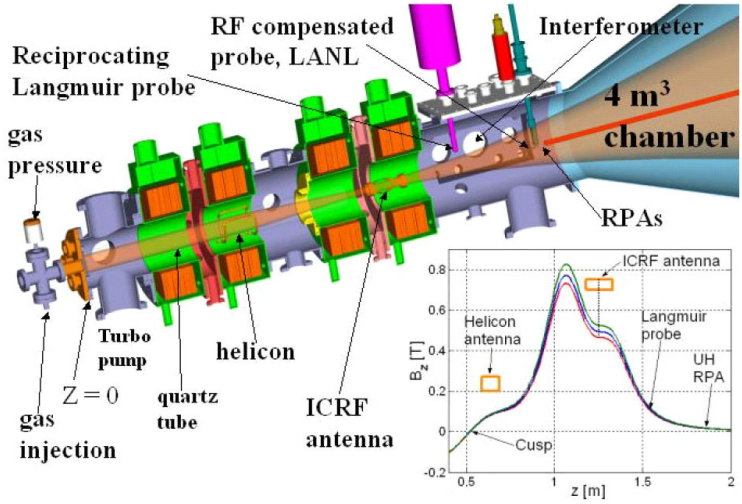

Figure 8. A trimetric view and axial field profile of the VX-10 device at JSC and associated diagnostics [17].

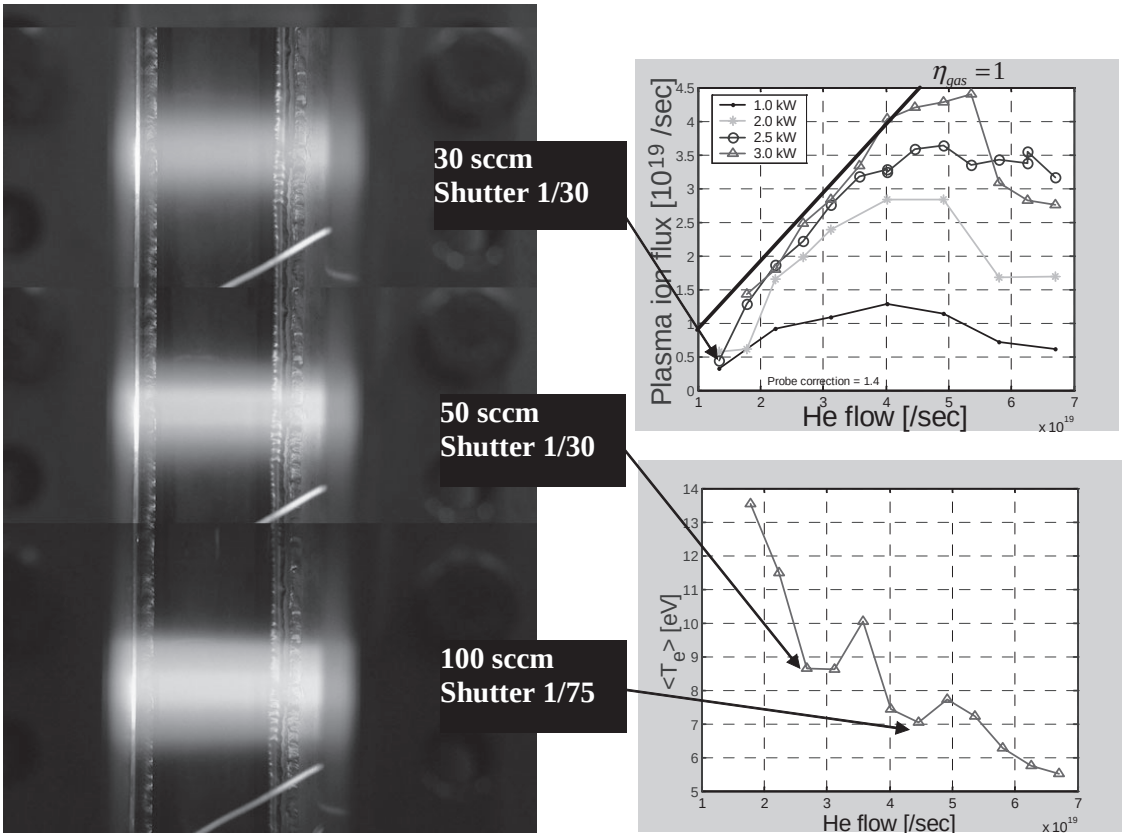

Figure 9. Plasma production and electron temperature as functions of the neutral-gas injection rate for helium. The discharge brightness at various flow rates is shown on the left. The visible color change and elevated electron temperature confirm neutral-gas depletion [17]

the CMA diagram), which approach the lower-hybrid resonance from the low-field side. The present helicon source has now been well characterized theoretically and experimentally, with hydrogen, helium, deuterium, and other propellants [53-55]. Stable plasma discharges are now routinely produced with densities in the 10^{18} to 10^{19} m^{-3} range. The present configuration features a 9-cm inner diameter helicon tube threaded through a water-cooled, double-saddle "Boswell" type antenna.

Unlike more conventional helicon discharges, used in plasma processing and other applications, the VASIMR source operates in a flowing mode, which requires careful control of the pressure field within the discharge tube. Discharges with nitrogen, argon, and xenon have also been studied, but data with these propellants are still rather sparse.

Nearly complete propellant ionization in the helicon tube has now been measured. This important result, relating to the ultimate propellant utilization efficiency of the device, is shown in Figure 9 [17, 56, 57]. In that figure, measured ion output and neutral-particle input fluxes are compared, and show a one-to-one correspondence in the range between 2×10^{19} and 4×10^{19} particles per second.

While the helicon is mainly a plasma-production stage, its operation produces non-negligible thrust. Direct measurements of the flow momentum have been carried out [58]. The standard 3 kW helicon discharge produces about 6-7 mN of force on a target placed a few centimeters away from the magnetic throat. The neutral propellant input rate (about 3×10^{-7} Kg/sec) leads to an I_{sp} estimate of about

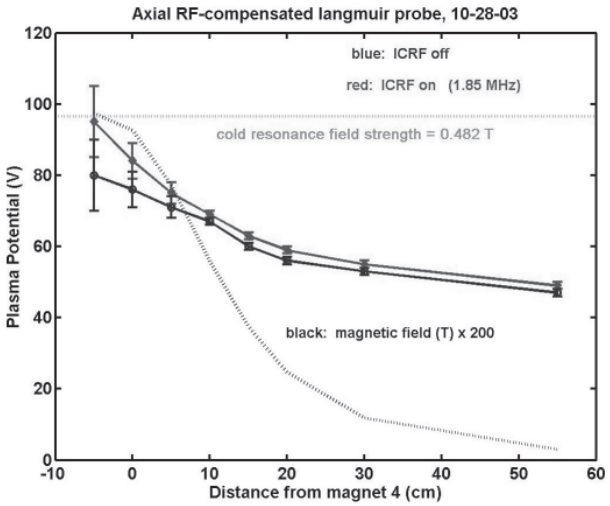

Figure 10. The profile of the plasma potential shows 30-50 V of potential drop between the ion-cyclotron resonant-frequency (ICRF) antenna and the retarding potential analyzer (RPA). The additional 30-50 V potential drop from the magnetic throat, B_{max}, is not shown [57].

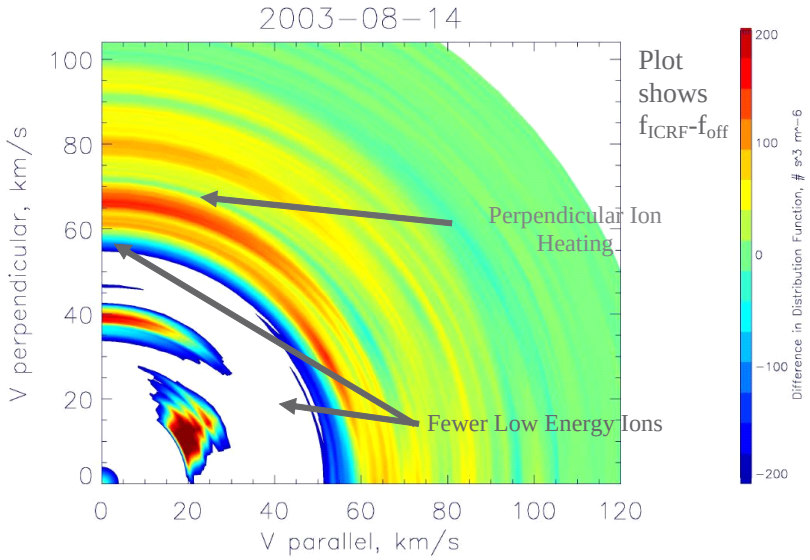

Figure 11. The difference in the velocity phase space distribution function between the ion-cyclotron resonant heating (ICRH) on and the ion-cyclotron resonant heating off conditions, plotted in spectrogram format using a linear color bar. The distribution has been mapped back to the location of the cyclotron resonance using conservation of the first adiabatic invariant. The perpendicular heating effect of the ion-cyclotron resonant heating shows up as the intense features at perpendicular velocities of 60-100 km/s [57].

2000 s. When the exhaust plasma is measured with a retarding potential analyzer (RPA) placed ~40 cm downstream from the momentum probe, the I_{sp} estimate increases to ~4000 s, with a corresponding increase in estimated thrust. We attribute this apparent acceleration to a combination of adiabatic (magnetic-mirror) acceleration and a 30-50 V ambipolar electrostatic potential drop, as shown in Figure 10. However, present pumping limitations increase the neutral background pressure downstream of the helicon throat, leading to collisions, which tend to reduce the flow momentum measured at the sensors; therefore, these measurements are presently only qualitative in nature.

Present experimental activities in the VASIMR project now focus on the physics of the RF booster, or ion-cyclotron stage. This stage is one of the unique features of the VASIMR system, in that it is the only magnetized electrode-less acceleration stage presently under development. The present configuration of the RF booster or ion-cyclotron resonant heating system uses 1.5 kW of 1.85 MHz left-hand-polarized slow-mode waves launched from the high-field, over-dense side of the resonance (region 13 of the CMA diagram). An important consideration involves the rapid absorption of ion cyclotron waves by the high-speed plasma flow. This process differs from the familiar ion-cyclotron resonance utilized in Tokamak fusion plasmas, as the particles in VASIMR pass under the antenna only once. Sufficient ion-cyclotron wave (ICW) absorption has nevertheless been predicted by recent theoretical studies [59, 60]. Recent experiments have confirmed these theoretical predictions with a number of independent measurements. What follows are brief highlights of some of these results [17, 56, 57].

The effect of the ion-cyclotron resonant heating is expected to be an increase in the component of the ion velocity perpendicular to the magnetic field. This increase will take place in the resonance region, i.e., the location where the injected RF wave frequency is equal to the ion-cyclotron frequency. Downstream of the resonance, this perpendicular heating will be converted into axial flow, owing to the requirement that the first adiabatic invariant of the particle motion be conserved as the magnetic field decreases. Since the total ion flux is not expected to increase, this axial acceleration should be accompanied by a density decrease. Furthermore, the particles should have a pitch angle distribution that does not peak at 0°. Instead, the distribution should peak at an angle that maps to a perpendicular pitch angle at resonance. Therefore, a collimated detector oriented along the magnetic field should observe a decrease in total flux and an increase in particle energy. As the acceptance angle of the detector is increased, the ion saturation current should start to show an increase when the acceptance cone includes the peak in the pitch-angle distribution.

An example of the distribution functions mapped back to the resonance that have been observed during ion-cyclotron resonant heating experiments is shown in Figure 11. During this particular experiment, the ion-cyclotron resonant-heating transmitter was operated at 1.85 MHz, at a power level of 1500 W. The data showed a pronounced enhancement or jet of ions with $v > 60$ km/s at 90° mapped pitch angle. The data also showed a depletion of ions with lower velocities. As shown in Figure 8, the magnetic-field intensity decreased rapidly with axial distance as one moved downstream away from the resonance region. At the location of the retarding potential analyzers, the field strength is down by a factor of ~40 from the value at the cyclotron resonance point. In a region like this, the effects of conservation of the first adiabatic invariant dominate ion dynamics. What conservation of the first invariant does is to force particles to lower and lower pitch angles as the field strength drops. This mechanism is the basis for the magnetic nozzle that makes the VASIMR an attractive design concept in the first place. A particle's pitch angle is given by

$$\theta = \arcsin\left(\theta_0 \sqrt{B/B_0}\right). \qquad (2)$$

A particle with a pitch angle of 90° at the resonance region will have a pitch angle of 10° at the location of the retarding potential analyzer. Thus all particles detected by the retarding potential analyzer at $\theta > 10°$ are either artifacts of the lack of collimation in the retarding potential analyzer, or particles that have been scattered or charge-exchanged. The effect of ion-cyclotron heating on the exhaust plasma is perhaps best illustrated by subtracting the "ion-cyclotron resonant heating off" distribution function from the "ion-cyclotron resonant heating on" distribution function and mapping the result back to the resonance region. The results shown in the figure are very dramatic. There was a clear depletion of low-energy ions and a significant enhancement of ions with perpendicular speeds > 60 km/s, exactly as predicted for ion-cyclotron resonant heating.

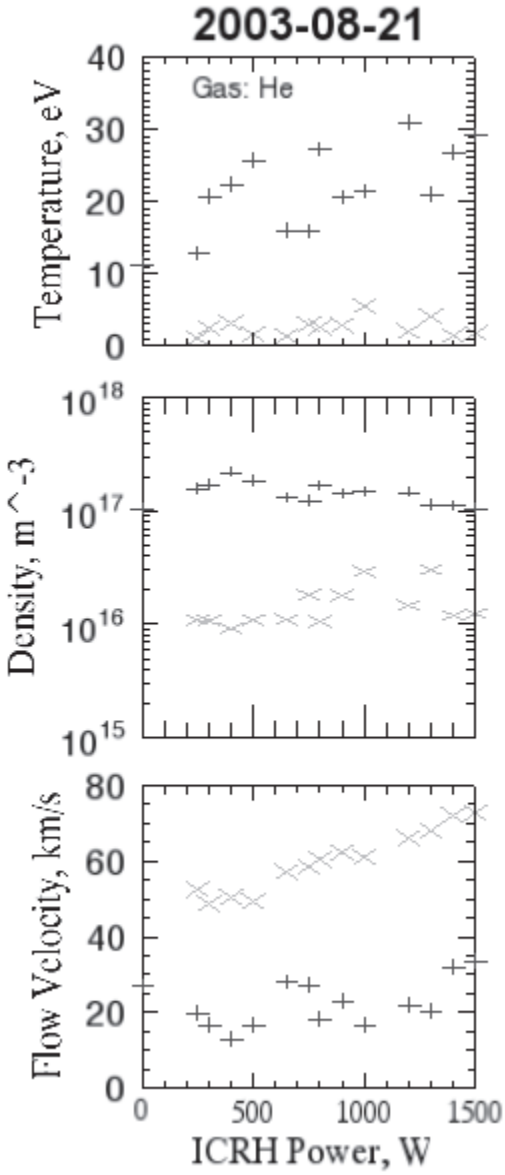

Figure 12. The fit parameters obtained by least squares fitting drifting bi-Maxwellian representations to the retarding potential analyzer data obtained during a scan of ion-cyclotron resonant heating transmitter power. From top to bottom, the panels show the ion drift velocity, the ion density, and the ion temperature in the frame of the beam. The plusses show the slow, hot component. The × marks show the fast, cold accelerated component. The round dots show the flow velocity expected for an energization rate of 70 eV/ion/kW of transmitted RF power.

The data indicates that the high remaining neutral background pressure in the present VASIMR test chamber produced a substantial amount of resonant charge exchange and scattering between the ion-cyclotron resonant heating antenna and the retarding potential analyzer location(s). The result was a pronounced "two-bump" distribution that is not well modeled by a single drifting Maxwellian. The data in Figure 11 strongly suggest using a bi-Maxwellian model, consisting of a hot, slow component and a fast component that has a low temperature in the moving frame.

The bi-Maxwellian model analysis has been used to interpret the results of a series of shots that scanned the ion-cyclotron resonant heating power input from 0 W to 1500 W. These results are presented in Figure 12. These results further strengthen the overall result of this paper, that the VASIMR VX-10 experiment is showing convincing evidence of single-pass ion-cyclotron resonant-frequency (ICRF) heating. The top panel shows that the accelerated beam had a low temperature in its reference frame, consistent with the expected output temperature of the helicon discharge. The temperature of the hot component was noisy. Generally, it was much hotter than the helicon output is expected to be, and the temperature increased with increasing ion-cyclotron resonant-heating power. The density of the accelerated component was 10-30% of the hot component, which is a measure of how much charge exchange and scattering was degrading the exhaust plume. We anticipate that the ratio of accelerated to scattered components will improve greatly with improved vacuum-pumping capacity. The flow velocity of the cold, fast component increased as the square root of input power, almost exactly in agreement with the value predicted for an energization rate of 70 eV/ion/kW of transmitted power. It is important to note that the team has barely begun the process of optimizing antenna coupling, and a substantial improvement in this performance is expected in the near future.

The ion-cyclotron resonant-heating RF booster in the VASIMR is the only known propellant-acceleration stage that is not restricted in power density by space-charge and beam-perveance effects. Furthermore, the use of an axial magnetic field allows erosion-free operation at much higher power and temperature levels than any other thruster. A 1 MW point design, suitable for use in a piloted mission to the outer planets, has been completed using technology that is presently available or feasible. The engine *alpha* parameter was just over 1 kg/kW. Thus, VASIMR has the unique advantage of being perhaps the only system discussed in

this paper that can be scaled to the requirements of a piloted mission without requiring prohibitively large thruster nozzle area.

3. Other RF Thrusters

The three systems that have been reviewed in detail here do not span the set of available RF- and microwave-using electric propulsion systems. Space does not permit detailed examination of all of the various concepts presently being explored. Some of the remaining ideas will be touched upon briefly.

3.1 Electrothermal Thrusters

Electrothermal thrusters operate by heating a gas electrically within a mechanically confined space and then releasing it through a conventional mechanical nozzle. The heating can be accomplished either by passage of a dc current through the gas, as in a resistojet or arcjet, or through microwave heating. The microwave electrothermal thruster (MET) has the advantage of not require erodable electrodes to be in contact with the heated propellant. Present microwave electrothermal thruster designs minimize discharge-chamber erosion by swirling the incoming propellant so as to confine the plasma to the center of the chamber, out of contact with the walls. The general advantage of the system is that it permits the use of inert, easily stored and common propellant materials, such as water. The systems under active development in the US are based on a design developed by Micci and coworkers at Pennsylvania State University [61-66]. Groups at Aerospace Corporation and Princeton have also contributed to the work [67-73]. These systems are intended for north-south station keeping on geosynchronous spacecraft. Most of the present generation of microwave electrothermal thrusters have I_{sp} values in the 200-400 s range, comparable to chemical systems. One Penn State system has reported an I_{sp} of 1330 s.

In an effort to develop higher I_{sp} systems, groups at Princeton and Stuttgart have begun to investigate the possibility of RF or microwave second-stage heating of electrothermal thrusters [68, 71, 72, 74]. These concepts are mostly in the numerical-modeling design phase at this time.

3.2 Ambipolar Thrusters

A number of efforts are underway to develop single-stage RF or microwave electric thrusters. Developers of these systems are trying to find a way to avoid using any gridded ion optics by using the generation of an ambipolar electric field in an axial magnetic field configuration. This approach offers two improvements over systems such as the RF ion thruster or microwave electron-cyclotron resonance thruster. The exhaust is comprised of neutral plasma instead of only ions, so no separate neutralizer cathode is required. There are no grids to erode and limit thruster lifetime. The principle of an ambipolar thruster is that a neutral exhaust requires ions and electrons to have the same exhaust velocity. The production of a hot electron gas in the ionization stage will lead to charge separation in the exhaust that is proportional to the electron pressure gradient. This violation of quasi-neutrality produces an electric field that acts to transfer energy from the electrons to the ions until the drift velocities equalize.

There are two initial ionization discharges that have been used in the development of an ambipolar thruster. The whistler-wave thruster used an approach of launching whistler waves (R mode) using a bifilar helical antenna surrounding an axial magnetic field [11, 12]. The waves propagated into a lower-field gas-injection region that contained the location of the electron-cyclotron resonance. The axial geometry contrasted with the ring cusp geometry of the microwave electron-cyclotron resonance thruster. The use of the whistler mode theoretically allowed the use of over-dense plasma. This system suffered from very high ion loss rates and low propellant utilization, owing to $\mathbf{E} \times \mathbf{B}$ drifts, and is no longer under active development.

The helicon discharge, on the other hand, is a robust, flexible heating mechanism that appears to offer an ideal source for an electrode-less ambipolar thruster. Gilland originally suggested adding a helicon discharge region to the whistler-wave thruster [13, 75, 76]. Subsequently, we reported on generation of thrust by the VASIMR light-ion helicon, operating in a stand-alone mode [48, 77]. Presently, groups at ISAS, NASA Glenn, and elsewhere have begun programs to examine the effectiveness of helicon discharges as thrusters [14, 15, 78].

3.3 Other

The only other system that uses an RF plasma discharge is the mini-magnetospheric plasma propulsion system [78-83]. This system utilizes a helicon discharge on inflate a locally produced magnetic field and create a mini-magnetosphere. The $\mathbf{j} \times \mathbf{B}$ force of the solar wind pushing on the mini-magnetosphere will then serve to provide 1-3 N of outward thrust on an interplanetary spacecraft. This system is controversial, and best suited to robotic missions to the outer planets.

4. Summary

Exploration of the solar system beyond Earth orbit is presently severely hampered by the limitations of chemical rockets. These limitations can only be removed by using electric power to provide additional energy and I_{sp} to the propellant. Given the presently available levels of electric power on spacecraft, high I_{sp} is achieved at the price of low thrust levels. These thrust levels mean that the thrusters must be able to operate reliably throughout missions of several years' duration. Electrodes and grids erode at the

elevated temperatures occurring inside electric thrusters. RF- and microwave-based systems offer a means to extend the lifetime of electric propulsion systems by avoiding the use of hollow cathodes, grids, and electrodes. Two systems have been space-qualified and lifetime rated to at least 18000 hours (~2 yr). Both of these systems have successfully operated in space for several thousand hours. RF-based systems also offer the opportunity to use neutral plasma exhaust instead of positive ions, thus obviating the need for a neutralizer cathode. Finally, one system, VASIMR, appears to offer the upward scalability to MW power levels required for human exploration of the outer planets.

5. Acknowledgements

NASA Johnson Space Center, under grant NAG 9-1524, and the Texas Higher Education Coordinating Board, under Advanced Technology Program project 003652-0464-1999, sponsored this research. The authors thank H. Bassner, K. Diamant, J. Foster, R. Killinger, H. Kuninaka, H. Leiter, M. Micci, and B. Stallard for reprints and figures.

6. References

1. K. Sankaran et al., "A Survey of Propulsion Options for Cargo and Piloted Missions to Mars," International Conference on New Trends in Astrodynamics, January 20-22, 2003.

2. F. R. Chang-Diaz, "Fast, Power-Rich Space Transportation, Key to Human Space Exploration and Survival," 53rd International Astronautical Congress/The World Space Congress, 10-19 October 2002, Houston, Texas, American Institute of Aeronautics and Astronautics.

3. F. R. Chang-Diaz et al., "Rapid Mars Transits With Exhaust-Modulated Plasma Propulsion," NASA Technical Paper 3539, 1995.

4. K. J. Hack, J. A. George, and L. A. Dudzinki, "Nuclear Electric Propulsion Mission Performance for Fast Piloted Mars Missions," AIAA/NASA/OAI Conference on Advanced SEI Technologies, September 4-6, 1991, Cleveland, OH.

5. S. N. Williams and V. Coverstone-Carroll, "Mars Missions Using Solar Electric Propulsion," *J. of Spacecraft and Rockets*, **37**, 1, 2000, pp. 71-77.

6. G. Saccoccia, J. Gonzalez del Amo, and D. Estublier, *Electric Propulsion: A Key Technology for Space Missions in the New Millennium*, 2000.

7. R. Killinger et al., "Electric propulsion system for ARTEMIS," 26th International Electric Propulsion Conference, IEPC, 1999, Kitayushu, Japan.

8. R. Killinger et al., "ARTEMIS Orbit Raising Inflight Experience with Ion Propulsion," 28th International Electric Propulsion Conference, IEPC 2003, Toulouse, France.

9. H. Kuninaka et al., "Development of Ion Thruster System for Interplanetary Missions," 23rd International Electric Propulsion Conference, IEPC 1993, Seattle, WA, USA.

10. K. Toki et al., "Flight Readiness of the Microwave Ion Engine System for MUSES-C Mission," 28th International Electric Propulsion Conference, IEPC 2003, Toulouse, France.

11. B. W. Stallard, E. B. Hooper, and J. L. Power, "Whistler-Driven, Electron-Cyclotron-Resonance-Heated Thruster: Experimental Status," *Journal of Propulsion and Power*, **12**, 1996, pp. 814-816.

12. B. W. Stallard, E. B. J. Hooper, and J. L. Power, "Plasma Confinement in the Whistler Wave Plasma Thruster," *Journal of Propulsion and Power*, **17**, 2001, pp. 433-440.

13. J. Gilland, "Application of a Helicon Discharge to Electric Propulsion," 34th Joint Propulsion Conference and Exhibit, 1998, Cleveland, OH.

14. R. Boswell and C. Charles, "The Helicon Double Layer Thruster," 28th International Electric Propulsion Conference, IEPC 2003, Toulouse, France.

15. K. Toki, "Preliminary Investigation of Helicon Plasma Source for Electric Propulsion Applications," 28th International Electric Propulsion Conference, IEPC 2003, Toulouse, France.

16. F. R. Chang-Diaz, "The VASIMR Engine," *Scientific American*, **283**, 5, 2000, pp. 72-79.

17. F. R. Chang-Diaz et al. "The VASIMR Engine: Project Status and Recent Accomplishments," 42nd Aerospace Sciences Meeting and Exhibit, 2004, Reno, NV, AIAA.

18. T. Froehlich, "RITA: High-Efficiency, Long-Life Radio-Frequency Ion Thrusters," EADS International Technology Days, 2003, Paris, France.

19. K. Groh and H. Loeb, "State of the Art of Radio-Frequency Ion Sources for Space Propulsion," *Review of Scientific Instruments*, **65**, 5, 1994, pp. 1741-1744.

20. H. Leiter et al., "Development and Performance of the Advanced Radio Frequency Ion Thruster RIT XT," 28th International Electric Propulsion Conference, IEPC 2003, Toulouse, France

21. R. F. Killinger et al., "RITA Ion Propulsion for ARTEMIS: Lifetime Test Results," 36th Joint Propulsion Conference and Exhibit, 2000, Huntsville, Alabama.

22. R. F. Killinger et al., "RITA Ion Propulsion for ARTEMIS – Results Close to the Completion of the Life Test," 37th Joint Propulsion Conference and Exhibit, Salt Lake City, Utah, 2001.

23. R. Killinger et al., "Results of the 15000 Hr Life Test of the RIT10 Ion Propulsion of ESA's ARTEMIS Satellite," 27th International Electric Propulsion Conference, IEPC 2001, Pasadena, CA, USA.

24. R. F. Killinger et al., "Electric propulsion system RITA for ARTEMIS," 35th Joint Propulsion Conference and Exhibit, 1999, Los Angeles, California.

25. H. Bassner et al., "Advantages and Applications of the RF-Ion Thruster RIT," 27th International Electric Propulsion Conference, 2001, Pasadena, CA.

26. R. F. Killinger et al., "Orbit Raising with Ion Propulsion on ESA's ARTEMIS Satellite," 38th Joint Propulsion Conference and Exhibit, 2002, Indianapolis, Indiana.

27.R. F. Killinger et al., "Final Report on the ARTEMIS Salvage Mission Using Electric Propulsion," 39th Joint Propulsion Conference and Exhibit, 2003, Huntsville, Alabama.

28.H. Bassner et al., "Development Steps of the RF-Ion Thrusters RIT," 37th Joint Propulsion Conference and Exhibit, 2001, Salt Lake City, Utah.

29.H. J. Leiter et al., "Development of the Radio Frequency Ion Thruster RIT XT," 27th International Electric Propulsion Conference, IEPC 2001, Pasadena. CA, USA.

30.H. J. Leiter et al., "Evaluation of the Performance of the Advanced 200 mN Radio Frequency Ion Thruster RIT XT," 38th Joint Propulsion Conference and Exhibit, 2002, Indianapolis, Indiana.

31.H. J. Leiter et al., "Extended Performance Evaluation of EADS ST's 200-mN Radio Frequency Ion Thruster," 39th Joint Propulsion Conference and Exhibit, 2003, Huntsville, Alabama.

32.H. Goede, "30 cm Electron Cyclotron Plasma Generator, *J. Spacecraft Rockets*, **24**, 1987, pp. 437-443.

33.H. Miyoshi et al., "Microwave Ion Thruster with Electron Cyclotron Resonance Discharge," 22nd International Electric Propulsion Conference, IEPC 1993**,** 1991, Viareggio, Italy.

34.J. E. Foster and M. J. Patterson, "Microwave ECR Ion Thruster Development Activities at NASA GRC," 38th AIAA Joint Propulsion Conference, 2002, Indianapolis, Indiana.

35.H. Kuninaka and S. Satori, "Development of Microwave Discharge Ion Thruster for Asteroid Sample Return Mission," 32nd AIAA Joint Propulsion Conference, 1996, Lake Buena Vista, FL.

36.H. Kuninaka et al., "Endurance Test of Microwave Discharges Ion Thruster Systems for Asteroid Sample Return Mission MUSES-C, 25th International Electric Propulsion Conference, IEPC 1997, Cleveland, OH, USA.

37.H. Kuninaka and S. Satori, "Development and Demonstration of a Cathodeless Electron Cyclotron Resonance Ion Thruster, *Journal of Propulsion and Power*, **14**, 1998, pp. 1022-1026.

38.H. Kuninaka et al., "Status on Endurance Test of Cathode-Less Microwave Discharge Ion Thruster," 34th AIAA Joint Propulsion Conference, 1998, Cleveland, OH.

39.H. Kuninaka et al., "Virtual Anode Phenomena Due to a Lack of Neutralization on Ion Thrusters Based on Muses-C Program," 37th AIAA Joint Propulsion Conference, 2001, Salt Lake City, UT.

40.K. Nishiyama et al., "Measurement of the Electromagnetic Emission from the MUSES-C Ion Engine System, 27th International Electric Propulsion Conference, IEPC 2001, Pasadena. CA, USA.

41.K. Toki et al., "Technological Readiness of Microwave Ion Engine System for MUSES-C Mission," 27th International Electric Propulsion Conference, IEPC 2001, Pasadena, CA, USA.

42.J. E. Foster and M. J. Patterson, "Discharge Characterization of 40 cm-Microwave ECR Ion Source and Neutralizer," 39th AIAA Joint Propulsion Conference, 2003, Huntsville, AL.

43.T. H. Stix, *Waves in Plasma*, New York, NY, American Institute of Physics, 1992.

44.I. Funaki et al., "20 mn-Class Microwave Discharge Ion Thruster," 27th International Electric Propulsion Conference, 2001, Pasadena, CA.

45.H. Toki et al., "Performance Test of Various Discharge Configurations for ECR Discharge Ion Thrusters," 27th International Electric Propulsion Conference, IEPC 2001, Pasadena. CA.

45a.H. Kuninaka, ISAS Press Release, 2003.

46.F. R. Chang-Diaz and T. F. Yang, "Design Characteristics of the Variable Isp Plasma Rocket AIDAA/AIAA/DGLR/JSASS," 22nd International Electric Propulsion Conference, October 14-17, 1991, Viareggio, Italy.

47.F. R. Chang-Diaz, "Research Status of the Variable Specific Impulse Magnetoplasma Rocket Open Systems," Transactions of Fusion Technology, July 27-31, 1998, Novosibirsk, Russia.

48.F. R. Chang-Diaz et al., "VASIMR Engine Approach to Solar System Exploration," The 39th AIAA Aerospace Sciences Meeting and Exhibit, January 8-11, 2001, Reno, NV.

49.F. R. Chang-Diaz and J. L. Fisher, "A Supersonic Gas Target for a Bundle Diverter Plasma," *Nuclear Fusion*, **22**, 8, 1982.

50.R. W. Boswell, "Very Efficient Plasma Generation by Whistler Waves Near the Lower Hybrid Frequency," *Plasma Phys. Control. Fusion*, **26**, 1984, p. 1147.

51.R. W. Boswell and F. F. Chen, "Helicons – The Early Years," *IEEE Transactions on Plasma Science*, **25**, 6, 1997, pp. 1229-1244.

52.M. D. Carter et al., "Radio Frequency Plasma Applications for Space Propulsion," International Conference on Electromagnetics in Advanced Applications (ICEAA99), 1999, Torino, Italy.

53.B. N. Breizman and A. V. Arefiev, "Ion Kinetics in a Magnetized Plasma Source, *Physics of Plasmas*, **9**, 3, 2002, pp. 1015-1024.

54.M. D. Carter et al., "Comparing Experiments with Modeling for Light Ion Helicon Plasma Sources," *Physics of Plasmas*, **9**, 12, 2002, pp. 5097-5110.

55.S. A. Cohen et al., "Ion Acceleration in Plasmas Emerging from a Helicon-Heated Magnetic-Mirror Device," *Physics of Plasmas*, **10**, 6, 2003, pp. 2593-2598.

56.F. R. Chang-Diaz et al., "Early Results of ICRH Experiments in VX-10," *Bulletin of the American Physical Society*, **DPP03**, 2003, p. RP1.138.

57.E. A. Bering, III et al., "Velocity Phase Space Studies of Ion Dynamics in the VASIMR Engine," 42nd AIAA Aerospace Sciences Meeting and Exhibit, 2004, Reno, NV, AIAA.

58.D. G. Chavers and F. R. Chang-Diaz, "Momentum Flux Measuring Instrument for Neutral and Charged Particle Flows, *Rev. Sci. Instrum.*, **73**, 10, 2002, pp. 3500-3507.

59.B. N. Breizman and A. V. Arefiev, "Single-Pass Ion Cyclotron Resonance Absorption," *Physics of Plasmas*, **8**, 3, 2001, pp. 907-915.

60. A. V. Arefiev, *Theoretical Studies of the VASIMR Plasma Propulsion Concept*, Austin, TX, The University of Texas at Austin, 2002, p. 119.

61. D. J. Sullivan and M. M. Micci, *Development of a Microwave Resonant Cavity Electrothermal Thruster Prototype*, 1993.

62. J. Mueller, J. and M. M. Micci, "Microwave Waveguide Helium Plasmas for Electrothermal Propulsion," *Journal of Propulsion and Power*, **8**, 1992.

63. P. Balaam and M. M. Micci, "Investigation of Free Floating Resonant Cavity Microwave Plasmas for Propulsion," *Journal of Propulsion and Power*, **8**, 1992.

64. P. Balaam and M. Micci, "Investigation of Stabilized Resonant Cavity Microwave Plasmas for Propulsion." *Journal of Propulsion and Power*, **11**, 1995.

65. D. J. Sullivan and M. M. Micci, "Performance Testing and Exhaust Plume Characterization of the Microwave Arcjet," 30th Joint Propulsion Conference. 1994, Indianapolis, IN.

66. F. Souliez et al., "Low-Power Microwave Arcjet Testing: Plasma and Plume Diagnostics and Performance Evaluation Micropropulsion for Small Spacecraft," in M. M. Micci and A. D. Ketsdever (eds.), AIAA, Reston, VA, 2000, pp. 199-214.

67. V. P. Chiravalle, R. B. Miles, and E.Y. Choueiri, "Numerical Simulation of Microwave-Sustained Supersonic Plasmas for Application to Space Propulsion," 39th AIAA Aerospace Sciences Meeting and Exhibit, 2001, Reno, NV.

68. V. P. Chiravalle, R. B. Miles, and E. Y. Choueiri, "Non-Equilibrium Numerical Study of a Two-Stage Microwave Electrothermal Thruster," 27th International Electric Propulsion Conference, 2001, Pasadena, CA.

69. K. D. Diamant, J. E. Brandenburg, and R. B. Cohen, "Performance Measurements of a Water-Fed Microwave Electrothermal Thruster," 37th AIAA Joint Propulsion Conference, 2001, Salt Lake City, Utah.

70. K. D. Diamant and R. B. Cohen, "High Power Microwave Electrothermal Thruster Performance on Water," 38th AIAA Joint Propulsion Conference, 2002, Indianapolis, IN.

71. V. P. Chiravalle et al., "Laser-Induced Fluorescence Measurements of a Two-Stage Microwave Electrothermal Thruster Plume," 34th AIAA Plasmadynamics and Lasers Conference, 2003, Orlando, FL.

72. V. P. Chiravalle, R. B. Miles, and V. P. Choueiri, "A Non-Equilibrium Numerical Study of a Microwave Electrothermal Thruster," 38th AIAA Joint Propulsion Conference, 2002, Indianapolis, IN.

73. K. D. Diamant, B. L. Zeigler, and R. B. Cohen, "Tunable Microwave Electrothermal Thruster Performance on Water," 39th AIAA Joint Propulsion Conference, 2003, Huntsville, AL.

74. S. Laure et al., "ATTILA-Adjustable Throttle Inductively Afterburning Arc Jet," 27th International Electric Propulsion Conference, 2001, Pasadena, CA.

75. J. Gilland, "The Potential for Compact Helicon Wave Sources for Electric Propulsion," 27th International Electric Propulsion Conference, 2001, Pasadena, CA.

76. J. Gilland, "Helicon Wave Physics Impacts on Electodeless Thruster Design," 28th International Electric Propulsion Conference, March 17-21, 2003, Toulouse, France.

77. E. A. Bering et al., "Experimental Studies of the Exhaust Plasma of the VASIMR Engine," 40th AIAA Aerospace Sciences Meeting & Exhibits, 14-17 January, 2002, Reno, NV.

78. R. M. Winglee, *Mini-Magnetospheric Plasma Propulsion (M2P2)*, Seattle, WA, University of Washington, 1999.

79. R. M. Winglee et al., "Mini-Magnetospheric Plasma Propulsion: Tapping the Energy of the Solar Wind for Spacecraft Propulsion," *Journal of Geophysical Research*, **105**, 2000, pp. 21067-21077.

80. R. M. Winglee et al., "Computer Modeling of the Laboratory Testing of Mini-Magnetospheric Plasma Propulsion (M2P2)," 27th International Electric Propulsion Conference, IEPC 2001, Pasadena, CA.

81. T. M. Ziemba et al., "Parameterization of the Laboratory Performance of the Mini-Magnetospheric Plasma Propulsion (M2P2) Prototype," 27th International Electric Propulsion Conference, IEPC 2001, 2001, Pasadena, CA.

82. R. M. Winglee et al., "Radiation Shielding Produced by Mini-Magnetospheres," Space Radiation Shielding Technology Workshop, 2002.

83. R. M. Winglee et al., "Simulation of Mini-Magnetospheric Plasma Propulsion (M2P2) Interacting with an External Plasma Wind," 39th AIAA Joint Propulsion Conference, 2003, Huntsville, AL.